PAPER • **OPEN ACCESS**

Glancing angle deposition of sculptured thin metal films at room temperature

To cite this article: S Liedtke *et al* 2017 *Nanotechnology* **28** 385604

OPEN ACCESS
IOP Publishing
Nanotechnology

Nanotechnology **28** (2017) 385604 (7pp)
https://doi.org/10.1088/1361-6528/aa7a79

Glancing angle deposition of sculptured thin metal films at room temperature

S Liedtke[1], Ch Grüner[1], A Lotnyk[1] and B Rauschenbach[1,2]

[1] Leibniz Institute of Surface Modification, Permoserstraße 15, D-04318 Leipzig, Germany
[2] Felix-Bloch Institute for Solid State Physics, University Leipzig, Linnéstr. 5, D-04103 Leipzig, Germany

E-mail: susann.liedtke@iom-leipzig.de

Received 5 May 2017, revised 9 June 2017
Accepted for publication 20 June 2017
Published 1 September 2017

Abstract

Metallic thin films consisting of separated nanostructures are fabricated by evaporative glancing angle deposition at room temperature. The columnar microstructure of the Ti and Cr columns is investigated by high resolution transmission electron microscopy and selective area electron diffraction. The morphology of the sculptured metallic films is studied by scanning electron microscopy. It is found that tilted Ti and Cr columns grow with a single crystalline morphology, while upright Cr columns are polycrystalline. Further, the influence of continuous substrate rotation on the shaping of Al, Ti, Cr and Mo nanostructures is studied with view to surface diffusion and the shadowing effect. It is observed that sculptured metallic thin films deposited without substrate rotation grow faster compared to those grown with continuous substrate rotation. A theoretical model is provided to describe this effect.

Keywords: glancing angle deposition, oblique deposition, sculptured metallic thin films, porosity, scanning electron microscopy, transmission electron microscopy

(Some figures may appear in colour only in the online journal)

1. Introduction

Glancing angle deposition (GLAD) [1] represents an elegant and simple technique for architecting a number of distinct nanostructure morphologies. Due to their versatility, these nanostructures cover numerous promising application areas such as sensing, energy and catalysis as well as biomedicine [2]. Although the field of GLAD has gained considerable interest during the last few decades [3–5], the knowledge about growth processes of metallic nanostructures prepared by GLAD remains incomplete.

In a common physical vapour deposition process, the angle θ between incoming particle flux and substrate normal is fixed close to 0°. However, modifying the angle θ represents an additional degree of freedom for influencing film morphology. Tilting the substrate to an oblique angle of incidence $\theta > 70°$ leads to the formation of a thin film consisting of separated tilted nanocolumns. This is called oblique angle deposition (OAD) [6, 7], whereas the combination of an oblique angle of incidence θ and simultaneous substrate rotation is called GLAD.

As the evaporated individual atoms reach the substrate surface, microscopic nuclei are formed so that the total surface energy of the nuclei is reduced. Other incoming atoms condense on these nuclei so that separated columns grow, which tend to broaden with increasing height [8]. In fact, not all nuclei will develop into high-aspect ratio columns, since the nucleation process is intrinsically random. In a competitive process, some columns will grow faster than other columns, resulting in a shadowing of the slower growing columns. As the substrate rotates, the apparent direction of the incoming particles is altered, which manipulates the shadowed regions and forces the columns to change their growth direction. Thus, a continuous substrate rotation allows the growth of spirals, screws, and upright columns depending on the rotation frequency [9–11]. A discrete substrate rotation can be also applied. Thereby, tilted columnar arms are grown during intervals without substrate rotation until the desired length of these arms is reached. Then, the substrate is rotated

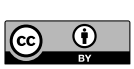

rapidly, which changes the growth direction of the next arm that is deposited atop the previous arm, etc. This technique opens the opportunity to fabricate complex n-fold chevron structures by implementing rapid, stepwise substrate rotations after growth intervals without substrate rotation.

Although several important conclusions concerning the influence of substrate rotation on the morphology of GLAD nanostructures have already been drawn, there are still open questions addressing this research topic. Detailed knowledge about growth mechanisms is relevant, because sub-μm scale morphology determines, for example, the plasmonic properties of such metallic nanostructured films considerably [12, 13]. An important issue is, for instance, the relationship between the angle of the incoming particle flux θ and tilt angle β of the grown nanostructures with respect to the substrate normal. Nieuwenhuizen and Haanstra [14] developed an empirical relation that describes the $\theta-\beta$ relation for angles of incidence below approximately 70°. For larger angles of incidence, the cosine rule proposed by Tait *et al* [15] reflects the $\theta-\beta$ relation for oblique angles ($\theta > 70°$) more appropriately. However, a large number of experimental results cannot be described successfully by those rules. A possible explanation is that tangent and cosine rules are derived from geometrical considerations, whereas further parameters influencing the growth of GLAD nanostructures are not considered. To overcome this, Tanto *et al* [16] proposed a semi empirical model based on the shadowing effect. This model summarizes the deposition and material parameters to one single parameter, the so-called fan angle, but it is unknown how the deposition and material parameters influence this fan angle. In this paper, the growth process of Al, Ti, Cr and Mo thin films prepared by GLAD at room temperature is studied. The selection of these metals covers a wide range of melting points. Since surface diffusion and melting point are correlated, a comparison between those metallic nanostructures reveals possible reasons for the significant differences obtained in growth behaviour. In addition, the influence of the substrate rotation on the columnar metallic nanostructures is discussed.

2. Experimental conditions

Metallic nanostructured films were grown by electron beam evaporation at a constant oblique angle of incidence θ of 84° between the incoming particle flux and substrates normal. The distance between the particle source (crucible) and substrate surface is approx. 30 cm. All depositions were done at room temperature (300 K) and at a working pressure of approx. 10^{-6} Pa. Planar Si(100) substrates with a thin native oxide film with a thickness that is typically in the order of a few nanometres were used for the experiments. The metals were chosen in a way that a wide range of melting points was covered: Al ($T_{melt} = 933$ K), Ti ($T_{melt} = 1941$ K), Cr ($T_{melt} = 2180$ K) and Mo ($T_{melt} = 2890$ K). A quartz crystal micro balance was used to control film height and deposition rate. All depositions were carried out at $\theta = 84°$ and with a deposition rate of 1 nm s^{-1}, except Mo, which had to be deposited with a rate of 0.5 nm s^{-1}. Computer-controlled substrate rotation allowed a precise and reproducible adjustment of film morphology. The grown nanostructured films were investigated by using a scanning electron microscope (SEM). Cross-sectional views of such films were obtained by cleaving the samples. Tilt angles of the columns with respect to the surface normal and the height of the nanostructured thin films were measured on the SEM images. To ensure a statistical reliability of the results, a considerable large number of SEM images were analysed. In addition, high resolution transmission electron microscopy (HR-TEM) utilizing a Titan^3 G2 60–300 microscope (300 kV) and selected area electron diffraction (SAED) were applied to analyse the microstructure of tilted Ti and Cr nanostructures and upright Cr nanostructures. TEM specimens were collected on Cu grids covered by lacey carbon by scratching the grid over the nanostructures, thus without using any solvents.

To compare metals with different melting points, the homologous temperature (T_H) is used. The homologous temperature is a well-proven and tested parameter to compare the morphology of different materials [17]. T_H is determined by scaling the substrate temperature T_{sub} (here always room temperature) to the melting point T_{melt} of the evaporated metal at standard conditions to $T_H = T_{sub}/T_{melt}$. The effect of pressure in a vacuum chamber on the melting point is very small and therefore negligible [18].

3. Results and discussion

3.1. Shaping of nanostructures

The experiments were carried out at room temperature and at constant deposition rate of 0.5 nm s^{-1} for Mo and 1 nm s^{-1} for Al, Ti and Cr. As shown in figure 1, tilted columns are created without substrate rotation, whereas substrate rotation frequencies from 0.03 rpm to 10 rpm represent an additional degree of freedom for modifying the shape of the generated nanostructures significantly.

For Mo, the shape of nanostructures varies from tilted columns over spirals and screws up to upright columns with increasing rotation frequency. This metal has a homologous temperature of $T_H = 0.1$ for deposition at room temperature and therefore the lowest T_H compared to the other metals. This low T_H is correlated with a strictly limited surface self-diffusion. Thus, the self-shadowing effect is maximal, resulting in the growth of high-aspect ratio rods.

In contrast to Mo, Cr and Ti have $T_H = 0.14$ and $T_H = 0.15$, respectively. Surface diffusion allows the incoming atoms to move into the shadowed regions. Thereby, the inter-shadowing effect is reduced, which leads to a smoothened surface of the grown nanostructures. Moreover, the columns tend to broaden in diameter while growing in height.

In contrast, for Al only upright columns can be created even though the substrate rotation frequency is modulated from 0.03 rpm to 10 rpm. Due to the low melting point, Al has at room temperature already $T_H = 0.32$ and hence a high surface self-diffusion. Thus, the incoming atoms can condense in the

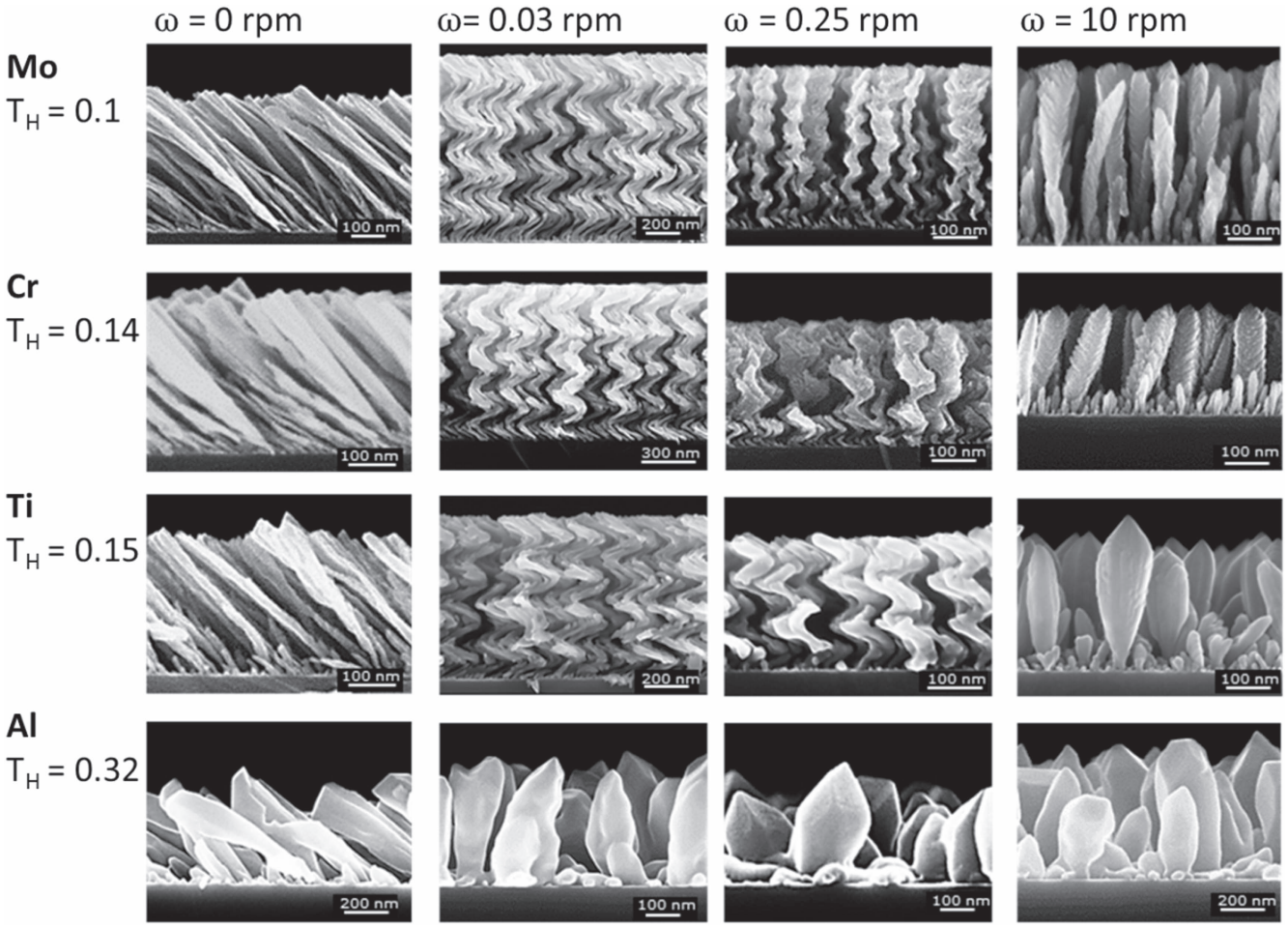

Figure 1. Cross-sectional SEM images of Al, Ti, Cr and Mo nanostructures deposited at room temperature with varying substrate rotation frequency ω (T_H is the homologous temperature).

shadowed regions so that the self-shadowing effect is smoothed out. Consequently, only upright Al columns can be grown with substrate rotation frequencies between 0.03 rpm and 10 rpm. Indeed, surface diffusion does not only influence the previously discussed shaping of the nanostructures, but also the area density and dimension of the seeds at the beginning of the deposition process, which should be considered. It can be noted that the shape of the grown metallic nanostructures after GLAD deposition at room temperature is strongly influenced by the rotation frequency and the homologous temperature.

3.2. Analysis of microstructure and morphology

Exemplarily, the microstructure of tilted Ti columns after deposition under an oblique angle of incidence of 84° at room temperature and at a deposition rate of 1 nm s^{-1} is analysed by HR-TEM and SAED. The results are presented in figure 2 and reveal a single crystalline structure of the tilted Ti columns. The crystal plane spacing is 0.233 nm, which corresponds to a *c*-axis oriented Ti nanostructure. The remaining diffraction reflection spots in figure 2 originate from the TiO_x oxide layer, which has a thickness of approximately 5 nm. Further, HR-TEM and SAED measurements on tilted Cr columns deposited at room temperature with a deposition rate of 1 nm s^{-1} show a single crystalline structure as well (figure 3) with a [110] growth direction. Hierarchical bundle-structures as described by the evolutionary columnar growth model developed by Messier *et al* [19] are not observed in the tilted Ti and Cr columns.

As the substrate is continuously rotated with 10 rpm, upright Cr columns are grown under oblique deposition ($\theta = 84°$), which are illustrated in figure 4. The HR-TEM and SAED patterns reveal polycrystalline morphology. Thereby, the preferred growth direction of the entire upright column Cr [110] is perpendicular to the substrate (along the column).

In summary, tilted Ti and Cr columns prepared at room temperature grow with single crystalline morphology, while upright Cr columns show polycrystalline morphology.

3.3. Influence of continuous substrate rotation

A continuous substrate rotation (ω = constant) in combination with oblique deposition under $\theta = 84°$ leads to sculptured thin films with spirals, screws, or upright columns (figure 1). To scale the height $h_{\theta=84°}$ of an obliquely deposited film to the height $h_{\theta=0°}$ of a film deposited vertically ($\theta = 0°$) for equal deposition times and deposition rates, scaling factors $F = h_{\theta=84°}/h_{\theta=0°}$ are used. In the case of oblique deposition,

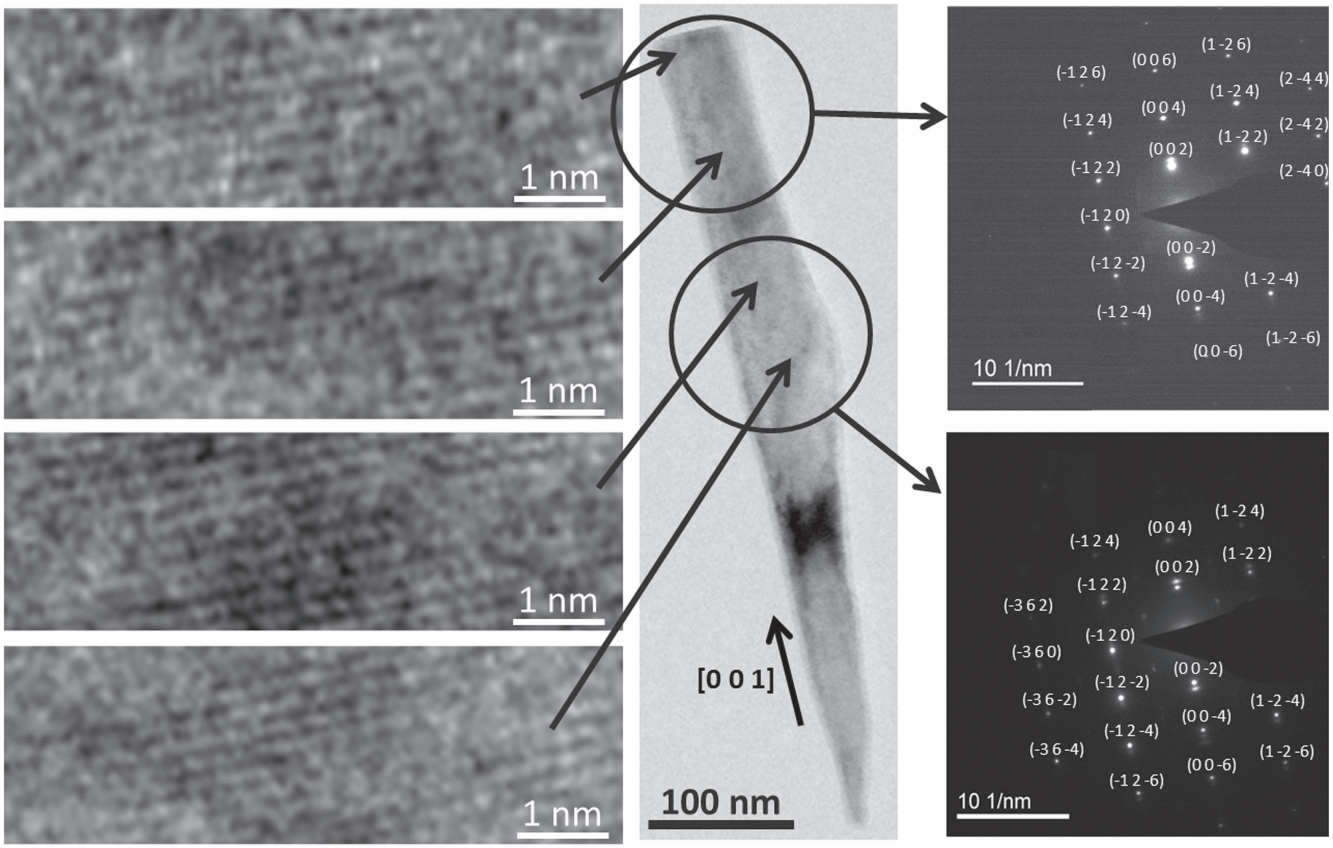

Figure 2. Bright-field TEM overview image (middle), HR-TEM images (left), and corresponding SAED patterns (right) of a tilted Ti column deposited at room temperature. Growth direction is parallel to [001].

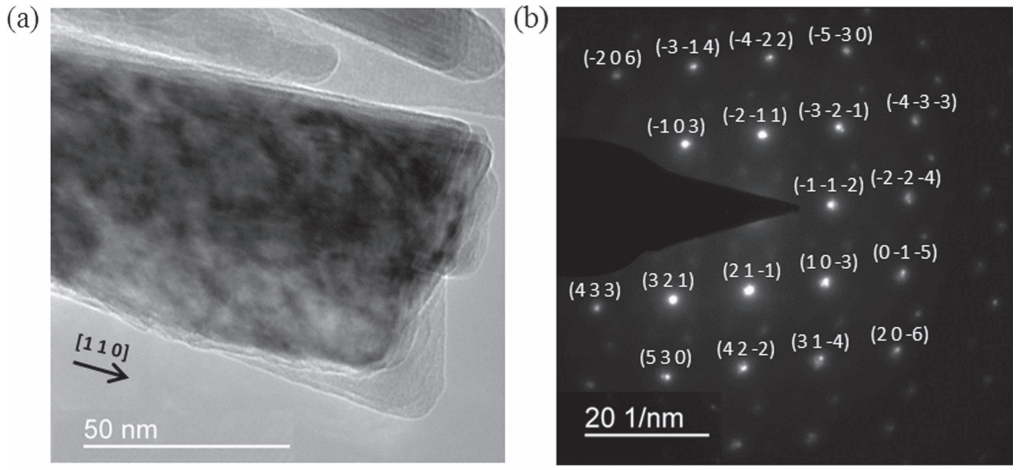

Figure 3. (a) Bright-field TEM overview image, and (b) corresponding SAED pattern of a tilted Cr column deposited at room temperature.

the scaling factor is $0 < F < 1$. For example, measuring the film height from SEM images for Ti films deposited obliquely ($\theta = 84°$) at room temperature and vertically for an equal deposition rate (1 nm s^{-1}) and deposition time yields a scaling factor of $F_{Ti} = 0.55$. This means, that the height of an obliquely deposited Ti film is reduced by a factor of 0.55 compared to the corresponding vertically deposited film. Consequently, after vertical deposition (parallel to the substrate surface normal) the film is characterized by a scaling factor $F = 1$.

Figure 5(a) shows the influence of the homologous temperature T_H on the scaling factors for the deposition of tilted and upright columns ($\theta = 84°$) with and without substrate rotation, respectively. Since all depositions are performed at room temperature, the corresponding T_H can be calculated for the evaporated metals to be $T_H = 0.1$ for Mo, $T_H = 0.15$ for Ti and $T_H = 0.32$ for Al. From figure 5(a), the following observations can be made: (i) the difference between the scaling factors by deposition with and without substrate rotation increases as T_H is enlarged, which suggests

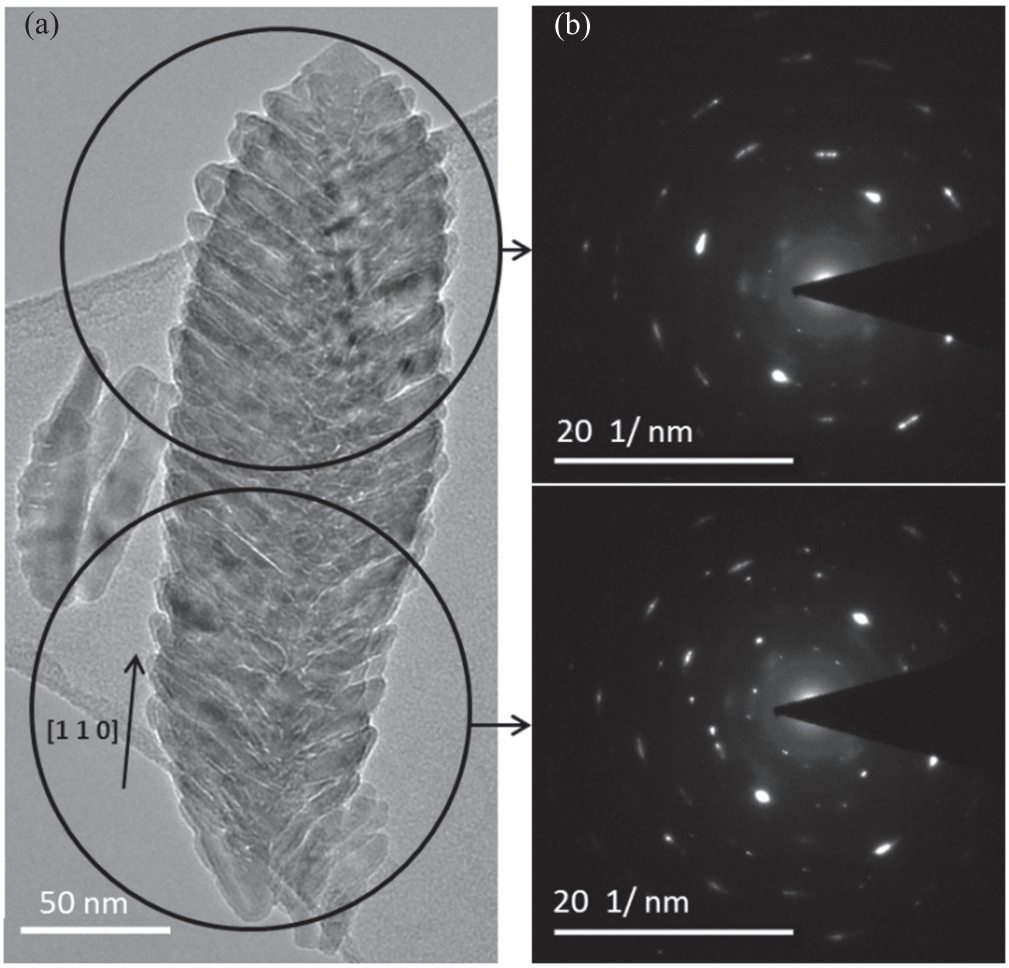

Figure 4. (a) Bright-field overview TEM image, and (b) corresponding SAED patterns of an upright Cr column deposited at room temperature.

that surface diffusion has a significant impact on the growth process. (ii) For equal deposition times and deposition rates, upright columns grow slower compared to tilted columns (figure 5(b)).

In the following, the pitch of screws and spirals is investigated. The so-called pitch [3] is defined as the deposited film height per one complete substrate revolution. To calculate which pitch would be expected if the screws and spirals would grow as fast as tilted columns, the scaling factor F is applied. Therefore, the scaling factors for the tilted columns $F_{Mo} = 0.64$, $F_{Ti} = 0.55$ and $F_{Cr} = 0.47$ are multiplied with the height $h_{\theta=0^\circ}$ of the vertically deposited film. Then, the expected pitch is compared with the measured pitch that is taken from the SEM images. The resulting plots are shown in figure 6. The orange graph illustrates the case if screws and spirals would grow as fast as tilted columns. Then, expected and measured pitch would be equal. However, the experimental results reveal that the measured pitch is smaller than the expected pitch, implying that screws and spirals grow slower than tilted columns, too. Aluminium screws and spirals are not analysed due to the high surface diffusion (see previous results under section (a)).

It should be noted that nanostructures grown with substrate rotation grow slower compared to those without substrate rotation. An explanation for this can be found with a view to the columnar microstructure. It has been shown before that e.g. tilted Cr columns grow single crystalline with a preferred growth direction along the titled column (see previous section (b)). Upright Cr columns are polycrystalline with a preferred growth direction perpendicular to the substrate (along the upright Cr column). However, in both cases the incoming particle flux is fixed to $\theta = 84^\circ$ with a constant deposition rate. Notice that these different preferred growth directions of tilted and upright columns influence the local deposition geometry of the growth zone of the nanostructures, which is discussed in the following.

The particle flux Φ defined as evaporated mass, m, per area, A, and time, t, according to Knudsen [20] is given by:

$$\frac{dm}{A\,dt} = \frac{M}{4\pi t}\frac{1}{r^2} \equiv \Phi, \qquad (1)$$

where M is the mass of the evaporated element and r is the distance between the evaporation source and the sample surface (here: 30 cm). The particle flux Φ can be measured directly by the quartz crystal micro balance. The grown film height h (measured parallel to the substrate normal) per time

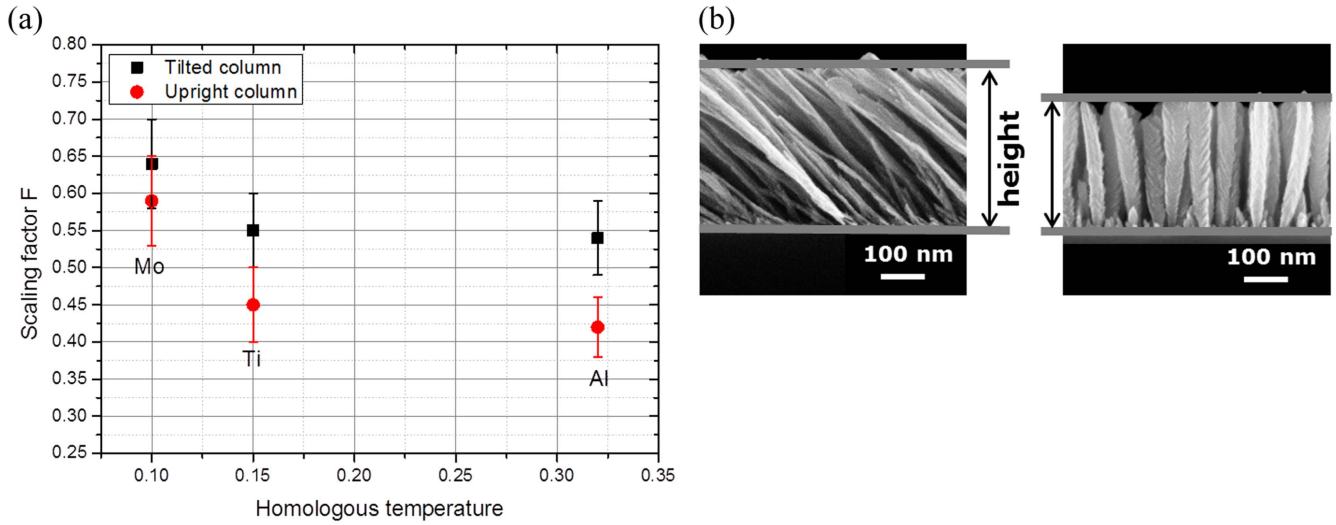

Figure 5. (a) Scaling factors for varying homologous temperatures. (b) Cross-sectional SEM images of tilted (left) and upright (right) Mo columns.

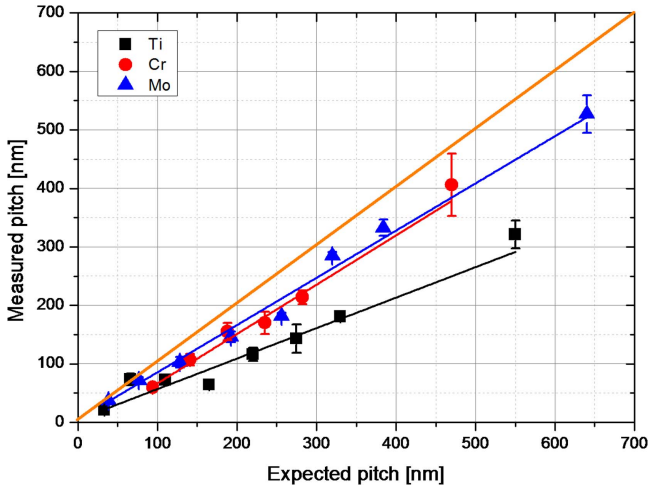

Figure 6. Expected versus measured pitch for screws and spirals.

t is given by the deposited mass m and the film density of the deposited material ρ, e.g., $dm/dt = A \cdot h \cdot \rho/t$. The film density ρ is defined by $\rho = \rho_0(1 - P)$, where ρ_0 is the density of the vertically deposited film ($\theta = 0°$) and P is the porosity. Notice that ρ_0 is not necessarily equal to the theoretical bulk film density, since the vertically deposited film could have inner voids, etc. Tilting the substrate to an oblique incidence angle θ results in the oblique angle deposition (OAD) geometry. Thereby, only a fraction of the evaporated atoms reduced by a factor of cos θ reaches the substrate so that the film height h_o can be assumed to:

$$h_o = \frac{\Phi \cdot t \cos(\theta)}{\rho} = \frac{\Phi \cdot t \cos(\theta)}{\rho_0 (1 - P)}. \quad (2)$$

For vertical deposition is $\theta = 0°$ and thus cos $(\theta) = 1$, whereas for oblique deposition is $\theta > 0°$ and cos $(\theta) < 1$. Consequently, the obliquely deposited film has a lower height compared to the vertically deposited film. However, the difference in film height between the obliquely and vertically deposited films is smaller than expected. This is due to the fact that the density of the deposited material of the film is decreased significantly as the substrate is tilted to oblique angles.

Upright columns grow parallel to the substrate normal with a growth zone that is oriented parallel to the substrate. In the case of upright columns the flux of particles reaching the growth zone is $\Phi_{parallel} = \Phi \cdot \cos(\theta)$, because the particle source is tilted by angle θ to the surface normal of the substrate. Consequently, the film height can be described by equation (2).

In contrast, for a tilted column the growth zone is no longer parallel to the substrate surface, since the growing surface is inclined to ($\beta - 90°$), where β is the angle between the surface normal and the growth direction of the column. Hence, the new angle of incidence, α, between incoming particle flux and normal of the growth zone is defined by $\alpha = \theta - \beta$. Thus, the particle flux Φ_{tilt} arriving at the tilted growth zone is $\Phi_{tilt} = \Phi \cdot \cos \alpha = \Phi \cdot \cos(\theta - \beta)$. Notice that the tilted columns grow in height with a factor of ($h/l = \cos \beta$), where h is the height and l is the length of the column. The growth in height for a tilted column is finally given by:

$$h_{tilt} = \frac{\Phi \cdot t \cos(\alpha) \cdot \cos(\beta)}{\rho}. \quad (3)$$

Hence, the trigonometrical term in (3) can be rearranged to give the following inequality:

$$\cos\theta < \cos(\alpha)\cos(\beta), \quad (4)$$

which can be proofed for $0° < \beta < \theta < 90°$. This condition is fulfilled for GLAD conditions and reflects the tendency of tilted columns to grow faster than screws, spirals and upright columns.

4. Conclusion

A variation of the substrate rotation frequency from 0.03 rpm to 10 rpm allows creating spirals, screws, and upright columns for Ti, Cr and Mo, whereas for Al only upright columns could be fabricated due to the high surface self-diffusion at

room temperature. Further, it was found that substrate rotation influences the microstructure of the column. In particular, this study has shown that tilted Ti and Cr nanostructures deposited at room temperature are single crystalline and show a preferred crystallite growth direction along the column, whereas upright Cr columns grow polycrystalline with a preferred growth direction perpendicular to the substrate. These different preferred growth directions for tilted and upright columns influence the local deposition conditions of the growing zone of the nanostructures. Tilted columns grow faster than spirals, screws and upright columns. To describe this observation, a theoretical model has been developed.

Acknowledgments

S Liedtke would like to thank the graduate school BuildMoNa and Ch Grüner gratefully acknowledges the funding of the DFG project RA 641/23-1.

References

[1] Young N O and Kowal J 1959 *Nature* **183** 104–5
[2] Srivastava S K, Shalabney A, Khalaila I, Grüner C, Rauschenbach B and Abdulhalim I 2014 *Small* **10** 3579–87
[3] Hawkeye M M, Taschuk M T and Brett M J 2014 *Glancing Angle Deposition of Thin Films* vol 1 ed A Willoughby *et al* (West Sussex: Wiley)
[4] Barranco A, Borras A, Gonzalez-Elipe A R and Palmero A 2016 *Prog. Mater. Sci.* **76** 59–153
[5] Zhou C M and Gall D 2008 *J. Appl. Phys.* **103** 014307
[6] Kundt A 1886 *Ann. Phys., Lpz.* **263** 59–71
[7] König H and Helwig G 1950 *Optik* **6** 111–24
[8] Karabacak T, Singh J P, Zhao Y P, Wang G C and Lu T M 2003 *Phys. Rev.* B **68** 125408
[9] Messier R, Venugopal V C and Sunal P D 2000 *J. Vac. Sci. Technol.* A **18** 1538–45
[10] Patzig C, Rauschenbach B, Erfurth W and Milenin A 2007 *J. Vac. Sci. Technol.* B **25** 833–8
[11] Robbie K, Friedrich L J, Dew S K, Smy T and Brett M J 1995 *J. Vac. Sci. Technol.* A **13** 1032–5
[12] Wang H H, Liu C Y, Wu S B, Liu N W, Peng C Y, Chan T H, Hsu C F, Wang J K and Wang Y L 2006 *Adv. Mater.* **18** 491–5
[13] Aizpurua J, Bryant G W, Ritcher L J, Garcia de Abajo F J, Kelly B K and Mallouk T 2005 *Phys. Rev.* B **71** 235420
[14] Nieuwenhuizen J M and Haanstra H B 1966 *Phillips Tech. Rev.* **27** 87–91
[15] Tait R N, Smy T and Brett M J 1993 *Thin Solid Films* **226** 196–201
[16] Tanto B, Ten Eyck G and Lu T M 2010 *J. Appl. Phys.* **108** 026107
[17] Thornton J A 1974 *J. Vac. Sci. Technol.* **11** 666–70
[18] Hall T 1995 *J. Phys. Chem.* **59** 1144–6
[19] Messier R, Giri A P and Roy R A 1984 *J. Vac. Sci. Technol.* A **2** 500–3
[20] Knudsen M 1909 *Ann. Phys.* **333** 75–130